Bioorganic Chemistry 91 (2019) 103118

Contents lists available at ScienceDirect

Bioorganic Chemistry

journal homepage: www.elsevier.com/locate/bioorg

Revealing synergistic mechanism of multiple components in *Stauntonia brachyanthera* Hand.-Mazz. for gout by virtual screening and system pharmacological approach

Qiong-qiong Hua[a,b], Ying Liu[a], Cai-hong Liu[a], Li Liu[a], Da-li Meng[a,b,*]

[a] School of Traditional Chinese Materia Medica, Shenyang Pharmaceutical University, Shenyang 110016, PR China
[b] Beijing Shijitan Hospital, Capital Medical University, Beijing Key Laboratory of Bio-characteristic Profiling for Evaluation of Rational Drug Use, Beijing 100038, PR China

ARTICLE INFO

Keywords:
Stauntonia brachyanthera
Network pharmacology
Gout
Molecular docking
GO analysis
KEGG pathway enrichment analysis

ABSTRACT

Stauntonia brachyanthera Hand.-Mazz. (SB), reported as a traditional Chinese medicine, displays a wide spectrum of interesting bioactivities, such as anti-inflammatory and analgesia. It is noteworthy that anti-gout effects of the components in SB have been reported. Hence, this study contributes to the prediction of promising active compounds and mechanisms for the treatment of gout. The active compounds with better oral bioavailability, and drug-likeness of SB were selected for further investigation by the approach of network pharmacology, molecular docking, gene ontology (GO) analysis, and Kyoto encyclopedia of genes and genomes (KEGG) pathway enrichment analysis, respectively. A total of 34 predicted targets and 98 compounds in SB were obtained. Sorted by structure types of compounds, phenylethanoid glycosides exhibited the best anti-gout activity, followed by phenolics and flavonoids. What's more, it was shown in the network analysis that Serine/threonine-protein kinase mTOR (mTOR), Mitogen-activated protein kinase 12 (MAPK12), tumor necrosis factor (TNF-α), Integrin alpha-4 (ITGA4) and Phosphatidylinositol 4,5-bisphosphate 3-kinase catalytic subunit gamma (PIK3CG) were the key targets with intensely interaction, which should be attached more attention for further study. The functional enrichment analysis indicated that SB probably produced the anti-gout effects by synergistically regulating many biological pathways, such as MAPK signaling pathway, PI3K-Akt signaling pathway, Toll-like receptor signaling pathway and NOD-like receptor signaling pathway, etc. In addition, C61, C67, C68 and C81 might be promising leading compounds with good molecular docking score. As a consequence, the active constituents and mechanisms based on data analysis were holistically illuminated, which was of vital importance to the development of new drugs for gout.

1. Introduction

Gout, a kind of crystalloid arthritis, is caused by the disorder of purine metabolism and/or the reduction of uric acid excretion in the body, the main symptom is mainly manifested as hyperuricemia and acute and chronic arthritis, which is induced by the accumulation of monosodium urate crystal (MSU) [1]. At present, the main drugs for clinical treatment of gout are non-steroidal anti-inflammatory drugs (NSAIDs), colchicine and corticosteroids, etc [2]. NSAIDs have gradually become the first line of treatment for acute gout, but some adverse effects including renal toxicity, gastrointestinal toxicity and gastrointestinal bleeding have emerged in the treating process of NSAID [3]. Colchicine, a commercial anti-gout drug, displayed shortcomings of therapeutic effect, such as gastrointestinal reactions, toxicity and poor tolerance [4]. As meanwhile, another approach to treat gouty disease is to lower the content of uric acid. However, allopurinol and benzbromarone, which inhibit the synthesis and excretion of uric acid, will result in allergic, sever hypersensitivity reactions, and nephropathy [5,6]. As a consequence, it is urgent to develop therapeutic drugs with clear curative effect and few toxic and side effects.

Traditional Chinese medicine (TCM) is a comprehensive medicinal system that has been used in clinical practice for thousands of years [7]. In recent decades, TCM has been widely used worldwide due to its moderate treatment effects and lower side effects [8]. *Stauntonia brachyanthera* Hand.-Mazz. (SB), an evergreen shrub belonging to the family of Lardizabalaceae, is mainly distributed in the southwest of China including Hunan, Guizhou and Guangxi provinces, which is well-known for delicious and nutritious fruits [9]. Definite medicinal values in the treatments of cancer, inflammation, pain, and diuretics have also been reported as the whole plant is used as a traditional Chinese medicine for

* Corresponding author at: School of Traditional Chinese Materia Medica, Shenyang Pharmaceutical University, Shenyang 110016, PR China.
E-mail address: mengdl@163.com (D.-l. Meng).

https://doi.org/10.1016/j.bioorg.2019.103118
Received 6 May 2019; Received in revised form 30 May 2019; Accepted 10 July 2019
Available online 12 July 2019
0045-2068/ © 2019 Elsevier Inc. All rights reserved.

thousands years, especially in the area of Dong ethnic minority [10]. What's more, the anti-gout effects of the components in SB has been revealed in our previous studies [10,11]. However, the bioactive compounds and their mechanisms for the anti-gout activity are still not illustrated.

Network pharmacology, combined with pharmacology and pharmacodynamics, is a novel research field which is implicated in the application of omics and systems biology-based technologies [12]. Based on the principle of "disease-gene-target-drug" interaction, network pharmacology systematically observes the intervention and influence of drugs on disease networks, and reveals the mystery of multi-molecular drugs synergistically acting on human body, which is the same as the theory of TCM, treating diseases from a holistic perspective, with multi-component, multi-pathway and multi-target synergy [13]. Besides, the combination of network pharmacology and rich experience in TCM is expected to transform the traditional approach of "one target, one drug" into a "network targets, multiple components" strategy [14]. It is also a promising method for discovering potential drugs from herbal medicine [15].

In this study, 98 compounds were isolated from the leaves, stems, peels and roots of SB in our laboratory. With oral bioavailability screening and drug-likeness evaluation, potential ingredients could be obtained and network pharmacology, molecular docking, GO analysis, as well as KEGG enrichment analysis were applied to investigate the bioactive constituents and underlying mechanisms of SB for the treatment of gout.

2. Material and methods

2.1. Plant material

Samples of *S. brachyanthera* were collected in Hunan Province by Shumo Mei, Huaihua Medical College in October 2009, and were identified by Professor Jincai Lu, School of Traditional Chinese Materia Medica, Shenyang Pharmaceutical University. A voucher specimen (NO.HLG-0910) was deposited in the School of Traditional Chinese Material Medica, Shenyang Pharmaceutical University.

2.2. Chemical ingredients database building

There is no database containing compounds from SB. Therefore, 98 compounds of SB were collected from the leaves, stems, peels and roots of SB isolated in our lab (as shown in S.1), including 50 triterpenoids, 7 phenylethanoid glycosides, 14 phenolics, 12 flavonoids, 7 phenylpropanoids and 8 others. All isolated compounds from SB were subjected to purity analysis by high performance liquid chromatography using YMC-Pack ODS-AQ (250 × 4.6 mmI.D., 5 μm) with the purity (HPLC) > 98.5%. All compounds were identified by MS and ^{1}H-, ^{13}C NMR spectrometry. It was finally lyophilized and stored in a −20 °C refrigerator. Two dimensional (2D) structures of the compounds were sketched using Chembiodraw 2014.

2.3. Prediction of oral bioavailability, drug-likeness

There are various kinds of compounds contained in SB, including triterpenoids, phenylethanoid glycosides, phenylpropanoids, phenolics and flavonoids, etc. But only bioactive compounds can contribute to clinical treatment. Thus, prior to the target prediction, compounds which have good absorption, distribution, metabolism, and excretion (ADME) were an important aspect of drug discovery. To streamline the virtual screening, ADME properties of all the 98 compounds were predicted to select active compounds using QikProp, version 3.0 of Schrodinger [16]. QikProp provides ranges for comparing properties of a particular molecule with 95% of known drugs. It also flags 30 types of reactive functional groups that may cause false positives in high-throughput screening (HTS) assays(*QikProp*; v 3.0; Schrodinger, LLC: New York, NY, USA, 2018).

2.4. Target fishing

Different protein associated with gout were collected from the following resources:

(1) Search for targets related to gout (ICD10: M10) from Therapeutic Target Database (TTD) (https://db.idrblab.org/ttd/)
(2) Universal Protein Database. The names of proteins and their ID were searched on Uniprot (https://www.uniprot.org/).
(3) RCSB Protein Data Bank. It was applied to convert Uniprot ID of targets to the ones which could be identified in PDB, and the structures of protein were obtained. (http://www.pdb.org/)
(4) Literatures. We could collect some significant targets from gouty related literatures.

Based on the above four methods, 34 distinct targets associated with gout were collected.

2.5. Compound-Target network construction

In order to understand the complex relationship between active compounds and potential targets, a visual network was established by SYBYL-X 2.0 and Cytoscape v3.5.0 [17]. This network was composed of node and edge. Nodes represented to the molecules (compounds and targets), while edges indicated the intermolecular interactions (compounds and targets interactions), namely, the connections between nodes.

2.6. Compounds-Target-Target network

"Compounds-Target-Target network" was established based on STRING analysis [18,19].

2.7. Gene Ontology (GO) analysis

Gene Ontology (GO) is a framework for the model of biology [20]. In this study, GO terms with P values < 0.05 and Benjamini < 0.05 were employed and the data were collected by the DAVID 6.8 (Database for Annotation, https://david.ncifcrf.gov/) prediction.

2.8. Compound-Target-Pathway network

Based on the results in DAVID database, the Cytoscape 3.5.0 software was used to construct the compound-target-pathway network. The characteristics of multiple components, multiple targets and multiple pathways of SB were revealed through the construction of network.

2.9. Molecular docking

To evaluate predicted targets, the crystal structures of candidate targets were downloaded from RCSB Protein Data Bank (http://www.pdb.org/) and embellished through the Sybyl-X (version 2.0, TRIPOS Inc.) software, including removing the ligands, adding hydrogen, removing water, optimizing and patching amino acids. Before docking, ChemBioDraw 3D was used to make three dimensional chemical structural formulas and energy minimizing for all the compounds, and saved in MOL2 format. Besides, a suitable method of evaluating the precision of a docking procedure was needed. The accuracy and consistency of the docking results model by Molegro Virtual Docker (MVD) were checked by comparing the best docking poses between the

Table 1
44 potential active compounds from *S. brachyanthera* (SB).

Comp.	Name	#Stars	PercentHumanOral Absorption	Rule Of Five	Rule Of Three	Structure
C31	3,23-dihydroxy-akebonic acid	0	96.118	0	0	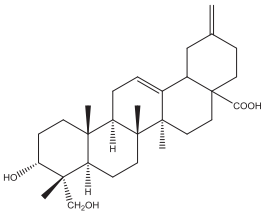
C32	3β-3-hydroxy-30-norolean-12,20(29)-dien-28-oic acid	0	90.197	1	1	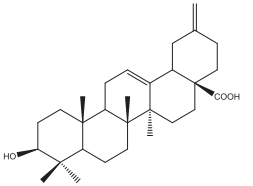
C33	3-*O*-α-L-arabinopyranosyl-akebonic acid	0	70.79	1	2	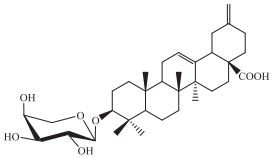
C34	3-O-α-L-rhamnopyranosyl-(1 → 2)-α-L-arabinopyranosyl-30-norolean-12,20(29)-dien-28-oic acid	3	32.444	3	1	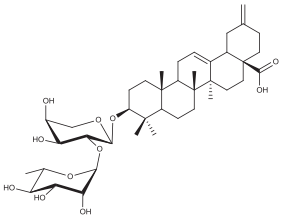
C36	Brachyanthera acid	0	26.19	2	1	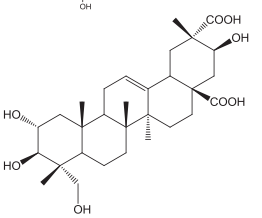
C37	Brachyanthera acid B	0	28.838	2	1	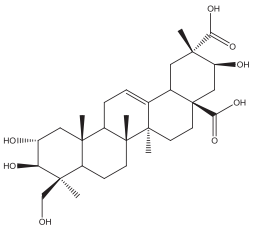

(*continued on next page*)

Table 1 (*continued*)

Comp.	Name	#Stars	PercentHumanOral Absorption	Rule Of Five	Rule Of Three	Structure
C38	Eupteleasaponin VIII	2	34.948	2	2	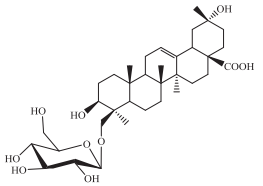
C42	Oleanolic acid	1	100	1	1	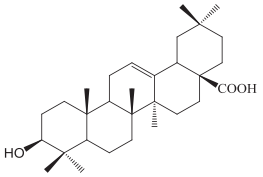
C43	3-acetoxy oleanolic acid	3	100	1	1	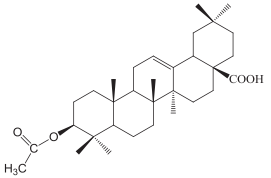
C44	Betulinic acid	1	96.076	1	1	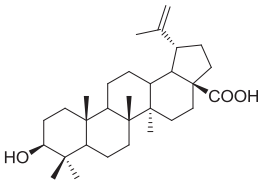
C45	Lupeol	4	100	1	1	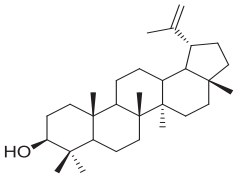
C46	16-β-hydroxylupane-20 (29)-en-3-one	2	100	1	1	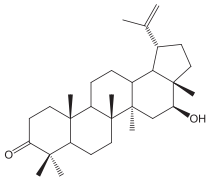
C47	Simiarenol	4	100	1	1	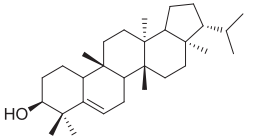

(*continued on next page*)

Table 1 (*continued*)

Comp.	Name	#Stars	PercentHumanOral Absorption	Rule Of Five	Rule Of Three	Structure
C48	Fernenol	4	100	1	1	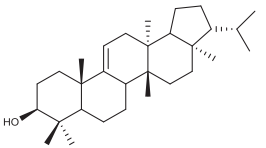
C49	*β*-sitosterol	5	100	1	1	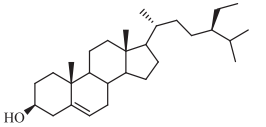
C50	Daucosterol	0	83.093	2	1	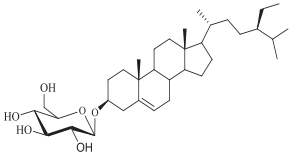
C54	Brachyanin D	1	25.321	2	1	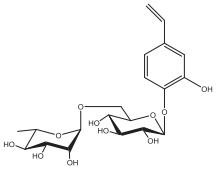
C57	(7*S*,8*S*)-S-yringylglycerol-8-*O*-*β*-D-glucopyranoside	2	29.445	2	1	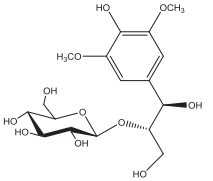
C58	4-*O*-*β*-D-(6-*O*-vanilloyl-glucopyranosyl) vanillic acid	0	32.25	1	1	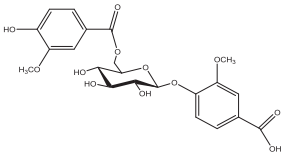
C59	4-O-(6-O-vanilloyl)- *β*-D-glucopyranosyl Vanillyl alcohol	0	50.62	1	1	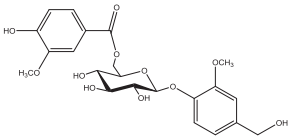
C61	1-*O*-*β*-D-(3,4-dihydroxyphenyl)ethyl-6-*O*-Vanilloyl glucopyranoside	0	26.625	2	1	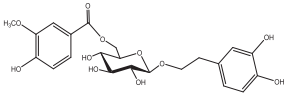
C64	2-(4′- hydroxyphenyl) ethyl-*β*-D -glucopyranoside	0	61.81	0	0	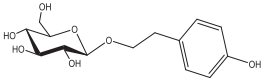

(*continued on next page*)

Table 1 (*continued*)

Comp.	Name	#Stars	PercentHumanOral Absorption	Rule Of Five	Rule Of Three	Structure
C65	2-(3′,4′-dihydroxyphenyl)ethyl-β-D-glucopyranoside	0	36.113	1	1	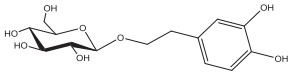
C66	erigeside C	0	60.277	0	1	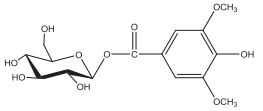
C67	1′-*O*-phenethyl-α-L-rhamnopyranosyl-(1 → 6)-β-D-glucopyranoside	0	50.552	1	1	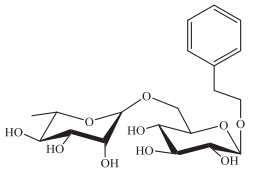
C68	ficuscarpanoside A	0	51.448	0	1	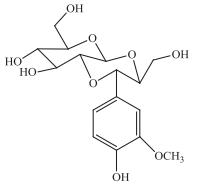
C69	ficuscarpanoside B	1	55.918	0	1	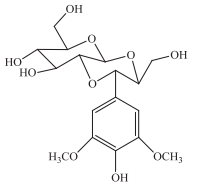
C70	kaempferol	0	64.845	0	0	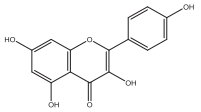
C72	quercetin	0	53.342	0	0	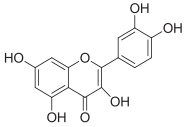
C75	vitexin	1	27.158	1	2	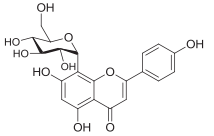
C81	licochalcone A	0	100	0	0	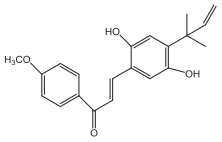

(*continued on next page*)

Table 1 (*continued*)

Comp.	Name	#Stars	PercentHumanOral Absorption	Rule Of Five	Rule Of Three	Structure
C83	staunoside C	1	40.687	3	1	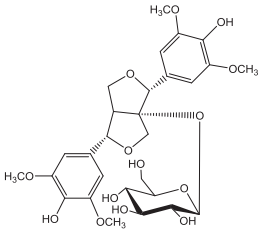
C84	7-(4-hydroxy-3-methoxyphenyl)-7′- (4′ - hydroxy-3′,5′-dimethoxyphenyl)-7,9′:7′,9-diepoxylignan-8H,8′-*O*-*β*-D-(2″,7′- epoxy)-glucopyranoside	1	44.404	2	1	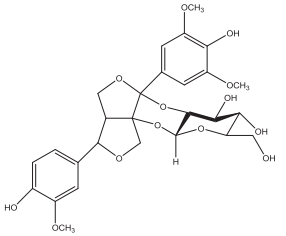
C85	Vanillic acid	0	67.481	0	0	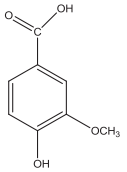
C86	Syringic acid	0	71.024	0	0	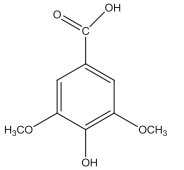
C87	Sinapaldehyde	0	82.937	0	0	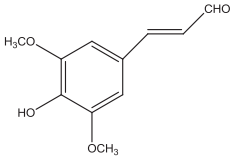
C88	Ferulyl aldehyde	0	81.34	0	0	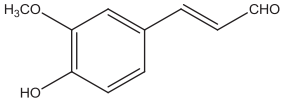
C89	Methyl chlorogenate	0	49.902	0	1	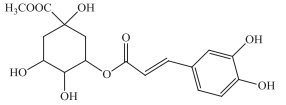

(*continued on next page*)

Table 1 (*continued*)

Comp.	Name	#Stars	PercentHumanOral Absorption	Rule Of Five	Rule Of Three	Structure
C90	Tortoside F	1	33.417	2	1	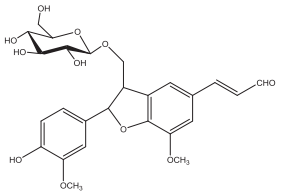
C91	Corchoionoside C	0	58.053	0	1	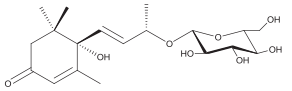
C92	2-methyl-4-pyrone-3-*O*-*β*-*D*-glucopyranoside	1	66.832	0	0	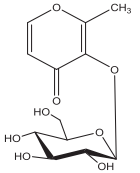
C93	3-hydroxy-2-methyl-4-pyrone	5	85.828	0	0	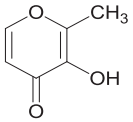
C97	*n*-butyl-*β*-D- fructopyranoside	0	71.047	0	0	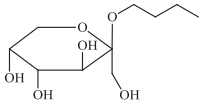
C98	Myoinositol	3	37.516	1	0	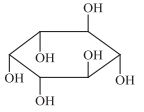

predicted conformation and the observed X-ray crystallographic conformation through the root mean square deviations (RMSDs). A model could be considered as reliable or accurate model when its RMSD was less than 3 Å (accurate ≤ 2 Å, reliable ≤ 4 Å) [21].

3. Results

3.1. Identification of active compounds

Among 98 compounds isolated from SB, 44 compounds were selected for their pharmaceutically significant ADME properties by using QikProp v3.0 tool of Schrodinger software. These properties are:

1. drug-likeness(#stars) (0–5)
2. Percent human oral absorption (> 80% is high, < 25% is poor)
3. Rule of five (maximum is 4)
4. Rule of three (maximum is 3)

All the selected structures and the ADME values of compounds were showed in Table 1. A large number of stars suggested that a molecule is less drug-like than molecules with few stars. The five rules were: molecular weight < 500, octanol/water partition coefficient < 5, estimated number of hydrogen bonds that would be donated by the solute to water molecules in an aqueous solution ≤ 5, estimated number of hydrogen bonds that would be accepted by the solute from water molecules in an aqueous solution ≤ 10. Compounds that satisfied these rules were considered as drug-like. The three rules were: aqueous solubility > −5.7, apparent Caco-2 cell permeability in nm/*sec* (Caco-2 cells are a model for the gut-blood barrier) > 22 nm/s, #primary metabolites < 7. Compounds with fewer (and preferably no) violations of these rules were more likely to be orally available. All ADME properties showed by selected compounds were in acceptable range.

3.2. Compound-Target network

By mapping 44 compounds to 34 potential targets which associated with purine catabolism, uric acid reduction, inflammation, and immune regulation, the interactions between compounds and targets were shown as Fig. 1a. Based on the docking results, the network embodied 76 nodes and 629 edges from Fig. 1a, in which colorized hexagon and circles corresponded to the targets and the compounds from SB, respectively. Degree is an important topological parameter that represent the performance of possible interactions between natural products and target proteins. The phenylethanoid glycosides, phenolics and flavonoids displayed more intimate association to most targets as shown in Fig. 1b, when docking with mTOR, MAPK12, TNF-α and PTGS2, etc.

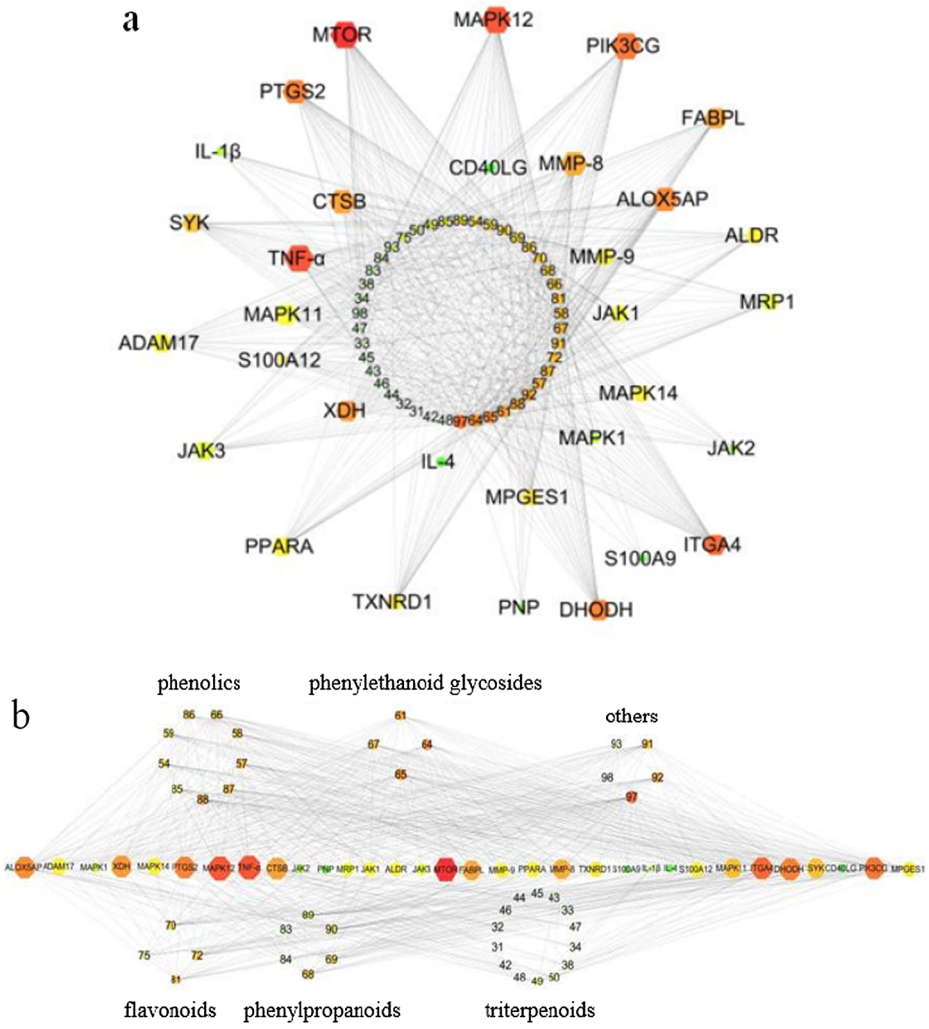

Fig. 1. Compound-target network of potential targets in *S. brachyanthera*. (a) The layout was according to the area and color of nodes: In a clockwise direction, the bigger and redder nodes were the ones with closer association. (b) The layout was according to skeleton type of compounds in order to find out the better ones with closer association.

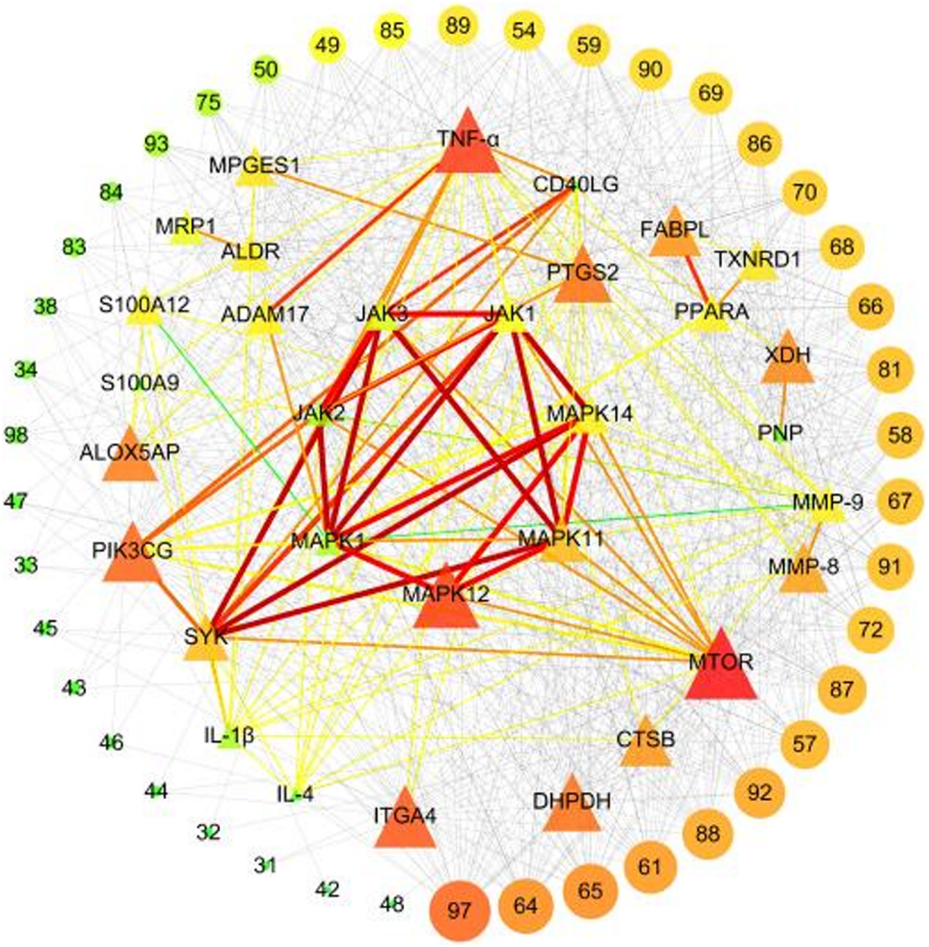

Fig. 2. Compound-target-target Network of potential targets in *S. brachyanthera*. The layout of outer ring is according to the area and color of nodes, which goes better in a clockwise direction. And the lines among inner nodes display the relationship between different proteins.

For example, C97 (degree = 29), C64 (degree = 26), C65 (degree = 26), C61 (degree = 25), C88 (degree = 24), C87 (degree = 23) and C81 (degree = 22), which might be of great importance in the treatment of gout. mTOR (degree = 35), MAPK12 (degree = 32), TNF-α (degree = 32), ITGA4 (degree = 30) and PIK3CG (degree = 29) might be the hub target of this network. Last but not least, in consistent with potential targets, more than half of the compounds displayed good docking performance, which was a good beginning for further research.

3.3. Compounds-Target-Target network

Based on the results of STRING for the interaction of targets, a "Compounds-Target-Target network" was built as described in Fig. 2, indicating some information of vital importance. On one hand, since coming from the same protein family, JAK1, JAK2 and JAK3 as well as MAPK1, MAPK11, MAPK12 and MAPK14 are related to each other, respectively. Furthermore, the JAK family is also closely related to the MAPK family, which indicating that a common pathway action may consists between these two families. On the other hand, more than half of the proteins are associated with TNF and IL-1β, demonstrating that most of the targets are anti-gout by acting with inflammatory targets. mTOR, SYK and PIK3CG associated with 11, 10 and 6 pivotal proteins, respectively, which play an important role in the treatment of gout diseases. Finally, DHODH was not associated with any protein, indicating that it does not function through the inflammatory pathway. With respect to compound structures, phenylethanoid glycosides corresponded to most gout-related targets, followed by phenolics and flavonoids.

3.4. GO analysis

A series of events accomplished by one or more organized assemblies of molecular function is described by the approach of GO biological process (GOBP). GOBP indicated that these targets were enriched to 17 biological process terms, and the 379 genes were highly related to regulation of apoptosis, response to organic substance, regulation of programmed cell death, regulation of cell death, regulation of cell proliferation, regulation of transcription from RNA polymerase II promoter and so on (as shown in Fig. 3).

3.5. Compound-Target-Pathway network

According to prediction of KEGG by DAVID 6.8, the Compound-Target-Pathway network was generated by the connection of potential pathways and corresponding targets (as shown in Fig. 4). The results showed that these predicted targets were intensively associated to the pathways as follows: MAPK signaling pathway, PI3K-Akt signaling pathway, NOD-like receptor signaling pathway, *T*-cell receptor signaling pathway, Toll-like receptor signaling pathway, Cytokine-cytokine receptor interaction, apoptosis and chemokine signaling pathway.

3.6. Molecular docking

The application of MVD and Discovery Studio software elucidated

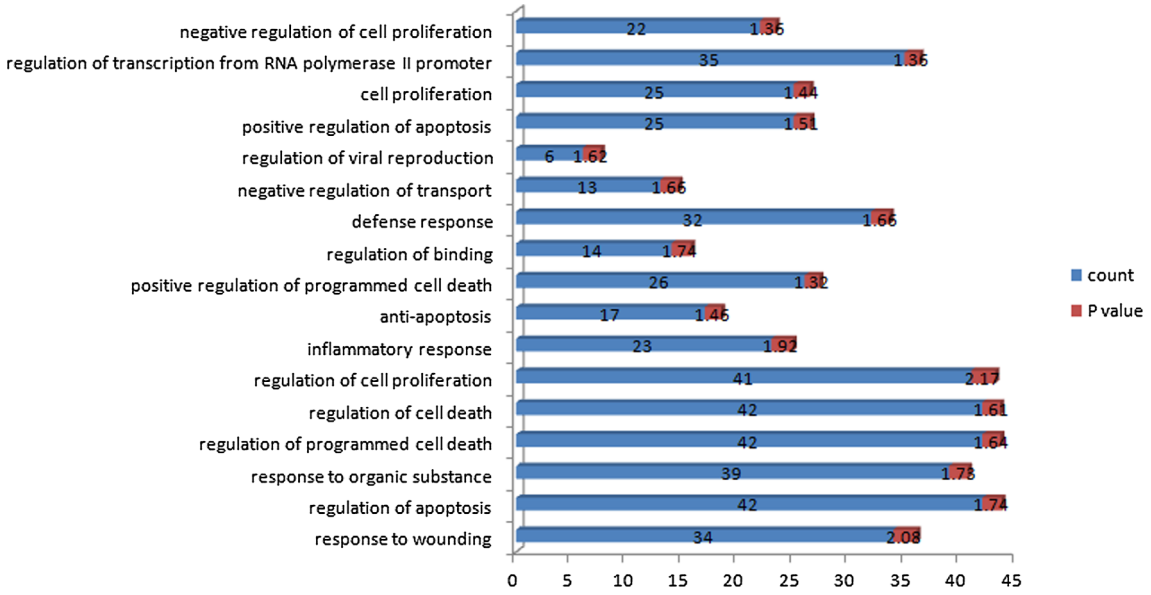

Fig. 3. GO biological process (GOBP) analysis. Counts of genes (blue) and − log10 P value (red) related to each biological process from DAVID 6.8 database.

the interactions between the potential active compounds (C57, C61, C64, C65, C67, C68, C69, C70, C72, C81, C87, C88, C92, C97) and the target proteins (mTOR, MAPK12, TNF-α, ITGA4, PIK3CG). The docking scores were depicted in Table.2. The smaller of docking score , the lower of energy would be required, which means the binding between the compounds and the targets are stronger. Compared with other compounds, the bonds among compound 61 and mTOR and ITGA4, compound 68 and MAPK12, compound 81 and TNF-α, compound 67 and PIK3CG have better performance.

The binding mode of C61 in the active site of mTOR had been

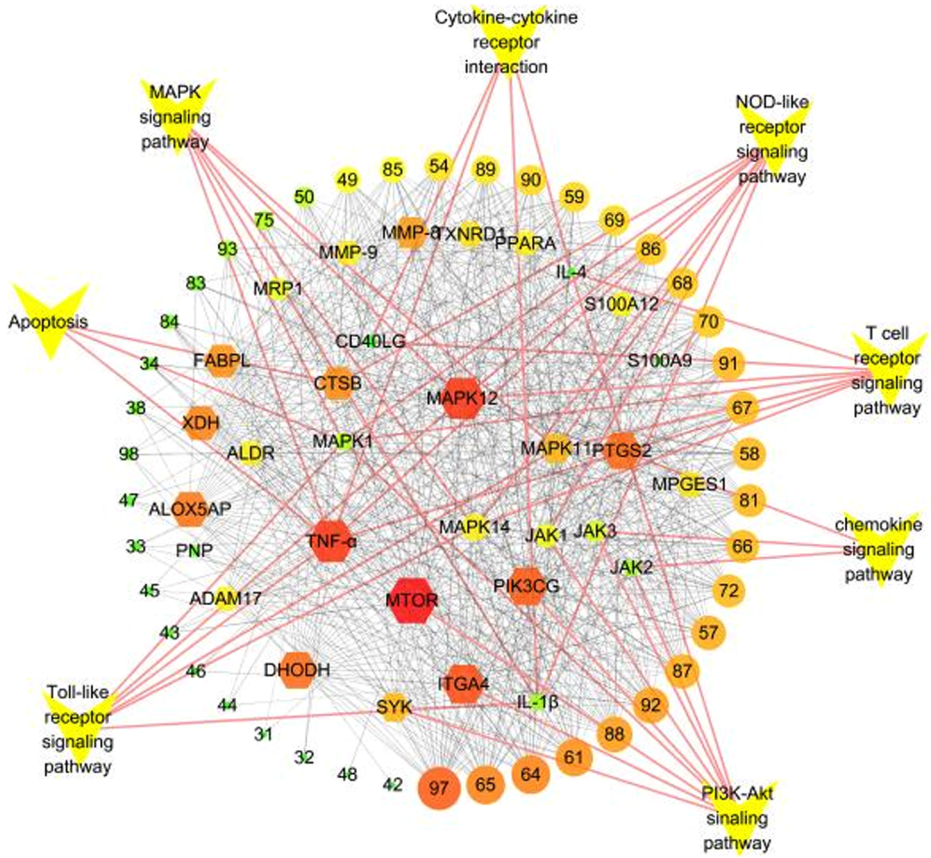

Fig. 4. Compound-target-pathway Network (C-*T*-P). Correspondence of shapes, lines and meanings was as follows: Colorized hexagon corresponds to potential target; Circle corresponds to compound; V corresponds to pathway; Pink line links pathway with target; Grey line links compound with target.

Table.2
Results of molecular docking studies of 14 compounds in the active sites of proteins (PDB ID 4JSV, 1CM8, 2AZ5, 3V4V and 6AUD) performed using Molegro Virtual Docker (MVD).

Compound	mTOR	MAPK12	TNF-α	ITGA4	PIK3CG
57	−97.4291	−62.4307	−92.986	−101.052	−111.692
61	−115.401	−82.1374	−84.8938	−119.623	−109.669
64	−77.3403	−40.9369	−87.2768	−80.4227	−91.4685
65	−79.2237	−59.2074	−96.0552	−85.4238	−101.691
67	−92.858	−56.9384	−77.3998	−81.5884	−117.476
68	−98.1934	−86.3587	−99.789	−96.7323	−105.894
69	−104.027	−68.7592	−110.195	−99.9112	−112.855
70	−92.3869	−52.7441	−90.6997	−87.1665	−88.7691
72	−93.4437	−58.5123	−95.2337	−96.4107	−92.4716
81	−108.432	−74.941	−113.066	−106.893	−111.929
87	−80.1814	−65.1362	−82.8364	−84.0199	−88.339
88	−81.8591	−62.2479	−89.04	−77.7552	−81.4496
92	−71.6531	−42.2502	−76.5185	−64.2364	−75.5164
97	−73.2459	−35.1967	−69.5969	−58.6041	−81.7152

represented in its three-dimensional mode in Fig. 5a while the schematic 2D dimensional representation had been shown in Fig. 5b. C61 showed seven H-bond interactions, among which four of them were phenolic hydroxyl with GLU 124, LYS 192 and SER 238. The other three, namely hydroxyl groups on glucose were with ASN 235 and PRO 196. Other interactions including Amide-Pi stacked, Pi-alkyl and Carbon Hydrogen Bond were connected with ASP 237 and LEU 236. In addition, the binding mode of C61 in the active site of ITGA4 had been represented in its three-dimensional mode in Fig. 5c and the schematic 2D dimensional representation had been shown in Fig. 5d. C61 showed five H-bond interactions, including a phenolic hydroxyl with ASN 235 residue, a methoxy group on the benzene ring with SER 238, and three were hydroxyl groups on glucose with SER 238. Another key residue which involved in interaction was GLU 240.

The binding mode of C68 in the active site of MAPK12 had been represented in its three-dimensional mode in Fig. 6e while the schematic 2D dimensional representation had been shown in Fig. 6f. C68 showed two H-bond interactions, one was a hydroxyl group with ARG 189 residue. The other one was the oxygen with ARG 192 residue. The other key residues which involved in interaction were ILE 197, HIS 231 and HOH 2086.

The binding mode of C81 in the active site of TNF-α had been represented in its three-dimensional mode in Fig. 6g and the schematic 2D dimensional representation had been shown in Fig. 6h. C81 showed three H-bond interactions as follows: carbonyl group from the flavonoid skeleton with TYR 151 residue and the C-OH group presented in the phenolic hydroxyl group on the B ring of flavonoid linked with GLY 121 and TYR 119 residue. Other key residues which involved in interaction were LEU 55, TYR 59 and TYR 119.

The binding mode of C67 in the active site of PIK3CG had been represented in its three-dimensional mode in Fig. 6i while the schematic 2D dimensional representation had been shown in Fig. 6j. C67 showed three H-bond interactions, including the hydroxyl group on glucose with LYS 890 residue and the hydroxyl group on rhamnose with ALA 885 and ASP 884. Another key residues which involved in interaction were TYR 867, MET 953, TRP 812 and HOH 1321.

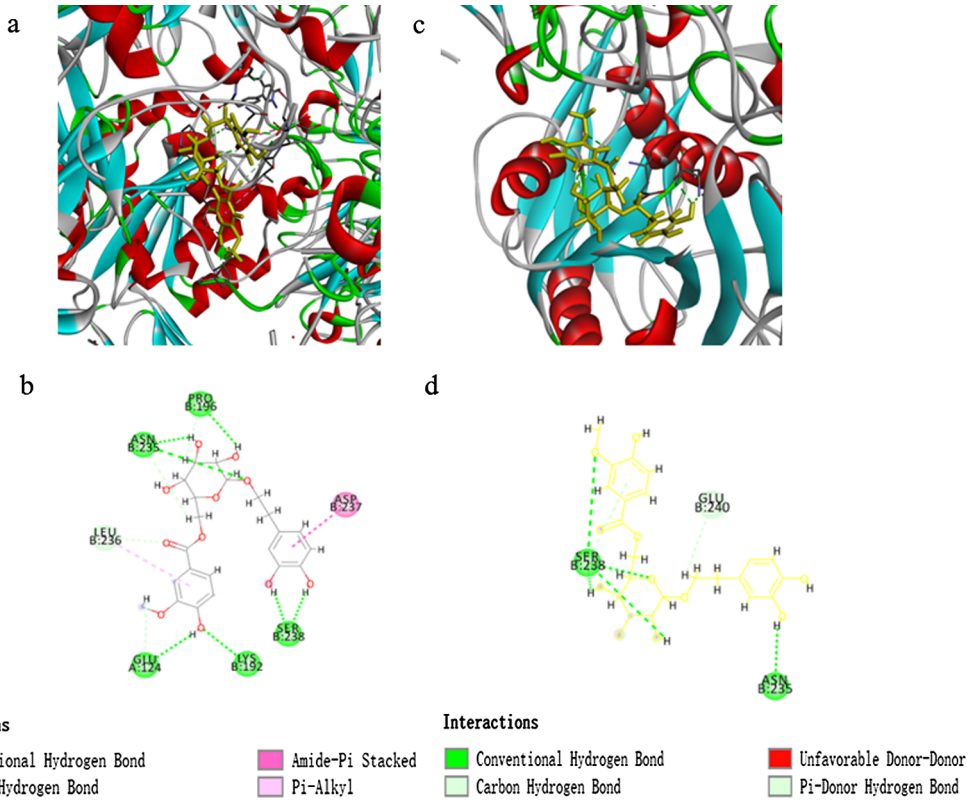

Fig. 5. (a) Schematic (3D) representation that molecular model of the compound 61 was in the protein mTOR (protein data bank ID chimeric 4JSV). Active site amino acid residues were represented as tubes, while the inhibitor was shown as stick model with yellow colored. (b) Schematic (2D) representation of interactions of compound 61 in the binding pocket of the protein. (c) Schematic (3D) representation that molecular model of the compound 61 was in the protein ITGA4 (protein data bank ID chimeric 3V4V). Active site amino acid residues were represented as tubes, while the inhibitor was shown as stick model with yellow colored. (d) Schematic (2D) representation of interactions of compound 61 in the binding pocket of the protein.

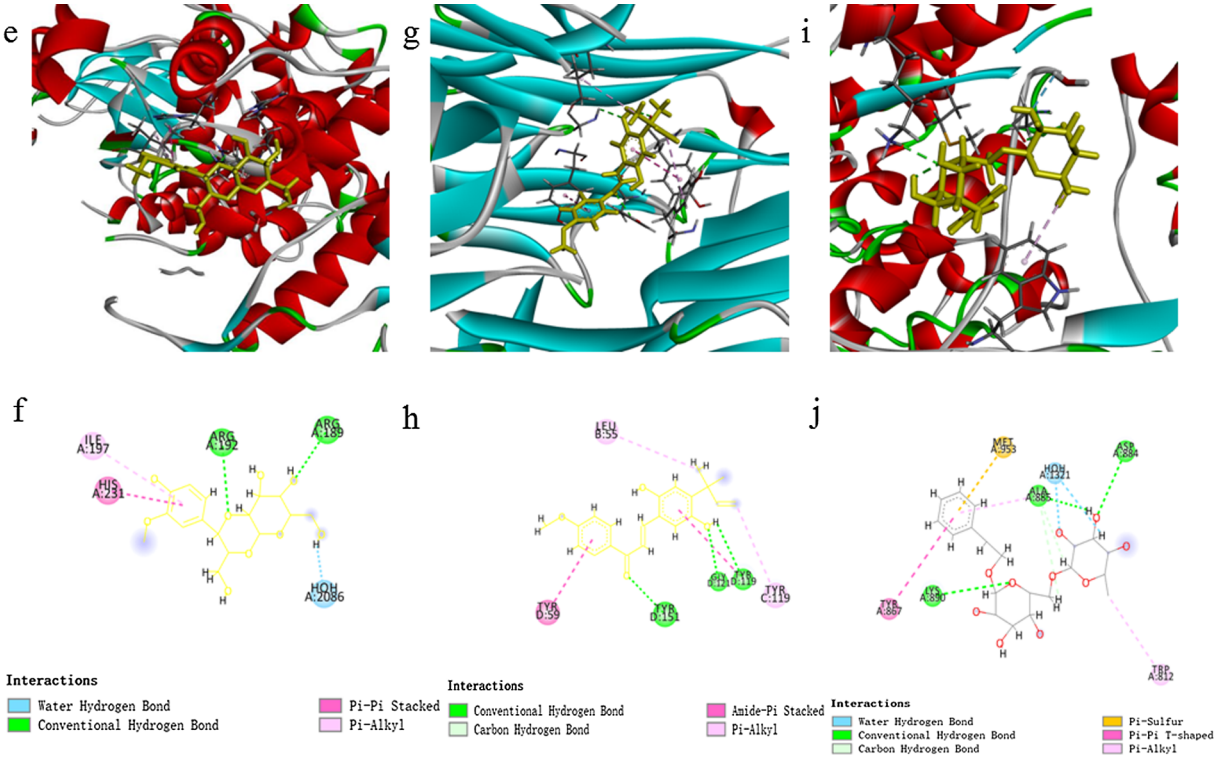

Fig. 6. (e) Schematic (3D) representation that molecular model of the compound 68 was in the protein MAPK12 (protein data bank ID chimeric 1CM8). Active site amino acid residues were represented as tubes, while the inhibitor was shown as stick model with yellow colored. (f) Schematic (2D) representation of interactions of compound 68 in the binding pocket of the protein. (g) Schematic (3D) representation that molecular model of the compound 81 was in the protein TNF-α (protein data bank ID chimeric 2AZ5). Active site amino acid residues were represented as tubes, while the inhibitor was shown as stick model with yellow colored. (h) Schematic (2D) representation of interactions of compound 81 in the binding pocket of the protein. (i) Schematic (3D) representation that molecular model of the compound 67 was in the protein PIK3CG (protein data bank ID chimeric 6AUD). Active site amino acid residues were represented as tubes, while the inhibitor was shown as stick model with yellow colored. (j) Schematic (2D) representation of interactions of compound 67 in the binding pocket of the protein.

4. Discussions

The application of network pharmacology to TCM provides new possibilities to understand the interactions among active compounds and relevant targets which highlight the mechanism of action [14,22].

In the study, we evaluated the active compounds and potential targets from SB against gout based on a systematic pharmacological method, including ADME-system assessment, Compound-Target network, Compound-Target-Target network, GO Analysis, Compound-Target-Pathway network and molecular docking. 44 active compounds were detected and interacted with 34 different targets associated with gout. According to the analysis of the Compound-Target network, sorted by structure types of compounds, it revealed that phenylethanoid glycosides exhibit the best anti-gout activity, subsequently followed by phenolics and flavonoids, which were consistent with the active ingredients reported in the previous literature for the treatment of gouty arthritis [23,24]. What's more, mTOR, MAPK12, TNF-α, ITGA4 and PIK3CG were the key factors in the compound-target interaction network.

With regard to the analysis of the Compound-Target-Target network, most proteins were more or less related, among which, the protein in the JAK family was the most strongly associated with the ones in the MAPK family. It revealed that the active compounds in SB might be used to treat gout through the pathways associated with these proteins. Interestingly, dihydroorotate dehydrogenase (quinone), mitochondrial (DHODH) is not associated with any protein, which is a mitochondrial enzyme that catalyzes the fourth step in the pyrimidine biosynthetic pathway, namely the conversion of dihydroorotate to orotate. DHODH inhibitors have anti-inflammatory and immunosuppressive effects and have been shown to be effective in the treatment of autoimmune diseases, such as, multiple sclerosis and rheumatoid arthritis [25]. It could be speculated that certain compounds in the SB had a similar effect as DHODH inhibitors for the purpose of treating gout.

The Gene Ontology (GO) project is a major bioinformatic approach to develop computational representation genes encode of biological functions at the molecular, cellular and tissue system levels. KEGG pathway enrichment analysis provides not only pathway functional annotations of given gene set but also pathway enrichment analysis. According to the results of GO and KEGG enrichment analyses, the targets were regulated by 379 genes correlated with multiple biological process and pathway, including MAPK signaling pathway, PI3K-Akt signaling pathway, NOD-like receptor signaling pathway, *T*-cell receptor signaling pathway, Toll-like receptor signaling pathway, Cytokine-cytokine receptor interaction, apoptosis and chemokine signaling pathway, which were intersecting, interacting, and synergetic.

4.1. MAPK signaling pathway

Mitogen-activated protein kinase (MAPK) signaling pathway is one of the important signal transduction systems *in vivo*, which is involved in the regulation of cell proliferation, differentiation, transformation and apoptosis through phosphorylation of nuclear transcription factors, cytoskeletal proteins and enzymes, and is closely related to the occurrence of various diseases such as inflammation and tumor. The signaling pathways of the MAPK family mainly include extracellular signal-regulated protein kinase (ERK), c-Jun *N*-terminal kinase (JNK),

p38 MAPK and ERK5/BMK [26,27]. Consistent with our data predictions, XU [28] found that Herba Siegesbeckiae improved the symptoms of gouty arthritis, whose possible mechanism was regulating the abnormal activation of JNK signaling pathway. Gout is a type of inflammatory arthritis induced by deposition of MSU in the joints and kidneys, where MSU crystals stimulate monocytesmacrophages and neutrophils to produce different pro-inflammatory cytokines, such as interleukin IL-1β, IL-6, tumor necrosis factor (TNF)-α [29]. Therefore, we speculated that the mechanism of the treatment of gout with SB is inhibiting the expression of inflammatory factors such as TNF-α, IL-1β, IL-6 induced by urate crystals, which could directly or indirectly activate the MAPK signaling pathway. SB might inhibit the occurrence of inflammatory reactions through the main target in MAPK signaling pathway, thereby getting rid of the occurrence of gout.

4.2. PI3K-Akt signaling pathway

As one of the important signal transduction pathways in the cell, the PI3K-Akt signaling pathway plays a key role in inhibiting apoptosis and promoting proliferation in the cell by affecting the activation state of various effector molecules downstream [30]. The PI3K-Akt signaling pathway is widely distributed in synovial tissue, which is related to synovial cell apoptosis, differentiation, adhesion, angiogenesis and matrix degradation, its overproduction can inhibit cell apoptosis [31]. In the pathogenesis of gout, IL-1β acts as the main inflammatory factor and activates many downstream signal transduction pathways [32]. YU [31] found that when gouty arthritis occurs, it stimulated the synthesis and release of IL-1β, which eventually activated AKT. PI3K-AKT is also involved in leukocyte chemotaxis, phagocytosis, inflammatory factor secretion and NF-kb activation in synovial inflammation, and plays a critical role in promoting synovial neovascularization and matrix degradation. The research indicated that total saponin of Dioscoreae Nipponicae Rhizoma (TSRDN) could inhibit fibroblast-like synoviocytes PI3K-AKT signaling pathway, and TSRDN had potential value in the treatment of gouty arthritis. Based on our predictions and previous studies, the PI3K-Akt signaling pathway might play an important role in the treatment of gout.

4.3. Other signaling pathway

Recent studies had shown that Toll-like receptor (TLR) and Nucleotide oligomerization domain-like receptor (NLR) were activated by exogenous or endogenous ligands, causing signal transduction cascade reaction, secretion of pro-inflammatory factors leading to not only inflammatory response, but also the occurrence of autophagy, what's more, autophagy has a significant negative regulation of inflammatory response to TLR, NLR signaling pathway [33]. Mutual regulation among autophagy, Toll-like receptor signaling pathway and NOD-like receptor signaling pathway may be of vital importance role in gout inflammation [34].

Combined with molecular docking results, C61, C67, C68 and C81 might be promising leading compounds with good molecular docking score. In addition, the docking results of phenylethanoid glycosides C61 and C67, phenylpropanoid C68 and flavonoid C81 were consistent with compound-target network pharmacology prediction, revealing that SB treated gout by multi-component synergy.

5. Conclusions

In conclusion, it was the first time to elucidate the mechanisms of action for SB for gout treatment by the approach of the virtual screening with systems pharmacology. Even though, further experiments are still demanded to validate our findings since this study was performed based on data analysis, it also contributes to searching for leading compounds and the development of new drugs for gout.

Targets abbreviations:

Number	PDB ID	Targets	Abbreviations
1	3O4O	Interleukin-1 beta	IL-1β
2	2CBZ	Multidrug resistance-associated protein 1	MRP1
3	3DZU	Peroxisome proliferator activated receptor gamma	PPARG
4	2E1Q	Xanthine dehydrogenase/oxidase	XDH
5	3VI8	Peroxisome proliferator activated receptor alpha	PPARA
6	5F19	Prostaglandin G/H synthase 2	PTGS2
7	1US0	Aldose reductase	ALDR
8	3VG7	Fatty acid-binding protein, liver	FABPL
9	4EAR	Purine nucleoside phosphorylase	PNP
10	2AZ5	Tumor necrosis factor	TNF-α
11	3D42	Mitogen-activated protein kinase 1	MAPK1
12	3GP0	Mitogen-activated protein kinase 11	MAPK11
13	1CM8	Mitogen-activated protein kinase 12	MAPK12
14	2FST	Mitogen-activated protein kinase 14	MAPK14
15	4JSV	Serine/threonine-protein kinase mTOR	mTOR
16	6AUD	Phosphatidylinositol 4,5-bisphosphate 3-kinase catalytic subunit gamma	PIK3CG
17	2D48	Interleukin 4	IL-4
18	1ALU	Interleukin 6	IL-6
19	3QFA	Thioredoxin reductase 1, cytoplasmic	TXNRD1
20	1A81	Tyrosine-protein kinase SYK	SYK
21	4GGF	Protein S100-A9	S100A9
22	2WCE	Protein S100-A12	S100A12
23	4AL0	Microsomal prostaglandin Esynthase 1	MPGES1
24	1ITV	Matrix metalloproteinase-9	MMP-9
25	1I76	Matrix metalloproteinase-8	MMP-8
26	5LWM	Tyrosine-protein kinase JAK3	JAK3
27	3UGC	Tyrosine-protein kinase JAK2	JAK2
28	3EYG	Tyrosine-protein kinase JAK1	JAK1
29	3V4V	Integrin alpha-4	ITGA4
30	4OQV	Dihydroorotate dehydrogenase (quinone), mitochondrial	DHODH
31	1ALY	CD40 ligand	CD40LG
32	3AI8	Cathepsin B	CTSB
33	2Q7M	Arachidonate 5-lipoxygenase-activating protein	ALOX5AP
34	2DDF	Disintegrin and metalloproteinase domain-containing protein 17	ADAM17

Declaration of Competing Interest

The authors declare no competing financial interest.

Acknowledgements

This work was supported by the National Natural Science Foundation of China (Grant No. 81573694, 81374061), and Open Research Funding of Beijing Key Laboratory of Bio-characteristic Profiling for Evaluation of Rational Drug Use (Grant No. 2018KF02).

Appendix A. Supplementary material

Supplementary data to this article can be found online at https://doi.org/10.1016/j.bioorg.2019.103118.

References

[1] K. Zhang, C. Li, Cytokines and gout: much learned, more to learn, Gout Hyperuricemia 2 (2015) 8–14.
[2] W. Chen, Y. Liu, M. Wei, L. Shi, Y. Wu, Z. Liu, S. Liu, F. Song, Z. Liu, Studies on effect of Ginkgo biloba L. leaves in acute gout with hyperuricemia model rats by using UPLC-ESI-Q-TOF/MS metabolomic approach, RSC Adv. 7 (2017) 42964–42972.
[3] E.P. Sabina, S. Nagar, M. Rasool, A role of piperine on monosodium urate crystal-induced inflammation–an experimental model of gouty arthritis, Inflammation 34 (2011) 184–192.
[4] G.C. Borstad, L.R. Bryant, M.P. Abel, D.A. Scroggie, M.D. Harris, J.A. Alloway, Colchicine for prophylaxis of acute flares when initiating allopurinol for chronic gouty arthritis, J. Rheumatol. 31 (2004) 2429–2432.

[5] S. Kumar, J. Ng, P. Gow, Benzbromarone therapy in management of refractory gout, New. Zeal. Med. J. 118 (2005) U1528.
[6] K.R. Hande, R.M. Noone, W.J. Stone, Severe allopurinol toxicity description and guidelines for prevention in patients with renal insufficiency, Am. J. Med. 76 (1984) 47–56.
[7] X. Liang, H. Li, S. Li, A novel network pharmacology approach to analyse traditional herbal formulae: the Liu-Wei-Di-Huang pill as a case study, Mol. BioSyst. 10 (2014) 1014–1022.
[8] F. Tang, Q. Zhang, Z. Nie, S. Yao, B. Chen, Sample preparation for analyzing traditional Chinese medicines, TrAC, Trends Anal. Chem. 28 (2009) 1253–1262.
[9] J. Zhao, J. Guo, Y. Zhang, D. Meng, Z. Sha, Chemical constituents from the roots and stems of *Stauntonia brachyanthera* Hand-Mazz and their bioactivities, J. Funct. Foods 14 (2015) 374–383.
[10] D. Liu, D. Wang, W. Yang, D. Meng, Potential anti-gout constituents as xanthine oxidase inhibitor from the fruits of *Stauntonia brachyanthera*, Bioorg. Med. Chem. 25 (2017) 3562–3566.
[11] X.L. Liu, S. Li, D.L. Meng, Anti-gout nor-oleanane triterpenoids from the leaves of *Stauntonia brachyanthera*, Bioorg. Med. Chem. Lett. 26 (2016) 2874–2879.
[12] F. Tang, Q. Tang, Y. Tian, Q. Fan, Y. Huang, X. Tan, Network pharmacology-based prediction of the active ingredients and potential targets of Mahuang Fuzi Xixin decoction for application to allergic rhinitis, J. Ethnopharmacol. 176 (2015) 402–412.
[13] Z. Liu, X. Sun, Network pharmacology: new opportunity for the modernization of traditional Chinese medicine, Acta Pharmaceutica Sinica 47 (2012) 696–703.
[14] F. Zhao, L. Guochun, Y. Yang, L. Shi, L. Xu, L. Yin, A network pharmacology approach to determine active ingredients and rationality of herb combinations of Modified-Simiaowan for treatment of gout, J. Ethnopharmacol. 168 (2015) 1–16.
[15] S. Hasan, B.K. Bonde, N.S. Buchan, M.D. Hall, Network analysis has diverse roles in drug discovery, Drug Discovery Today 17 (2012) 869–874.
[16] S. Chacko, S. Samanta, Novel thiosemicarbazide hybrids with amino acids and peptides against hepatocellular carcinoma: a molecular designing approach towards multikinase inhibitor, Curr. Comput. Aided Drug Des. 11 (2015) 279–290.
[17] P. Shannon, A. Markiel, O. Ozier, N.S. Baliga, J.T. Wang, D. Ramage, N. Amin, B. Schwikowski, T. Ideker, Cytoscape: a software environment for integrated models of biomolecular interaction networks, Genome Res. 13 (2003) 2498–2504.
[18] C. von Mering, L.J. Jensen, B. Snel, S.D. Hooper, M. Krupp, M. Foglierini, N. Jouffre, M.A. Huynen, P. Bork, STRING: known and predicted protein-protein associations, integrated and transferred across organisms, Nucl. Acids Res. 33 (2005) D433–D437.
[19] J. Xue, Y. Shi, C. Li, H. Song, Network pharmacology-based prediction of the active ingredients, potential targets, and signaling pathways in compound Lian-Ge granules for treatment of diabetes, J. Cell. Biochem. 120 (2019) 6431–6440.
[20] Z. Song, F. Yin, B. Xiang, B. Lan, S. Cheng, Systems pharmacological approach to investigate the mechanism of *Acori Tatarinowii Rhizoma* for Alzheimer's Disease, Evid Complement Alternat. Med. 2018 (2018) 5194016.
[21] A. Rayan, New tips for structure prediction by comparative modeling, Bioinformation 3 (2009) 263–267.
[22] W. Tao, X. Xu, X. Wang, B. Li, Y. Wang, Y. Li, L. Yang, Network pharmacology-based prediction of the active ingredients and potential targets of Chinese herbal Radix Curcumae formula for application to cardiovascular disease, J. Ethnopharmacol. 145 (2013) 1–10.
[23] M. Umamaheswari, K. AsokKumar, A. Somasundaram, T. Sivashanmugam, V. Subhadradevi, T.K. Ravi, Xanthine oxidase inhibitory activity of some Indian medical plants, J. Ethnopharmacol. 109 (2007) 547–551.
[24] Y. Xu, L. Xu, J. Liu, W. Fei, H. Nian, Studies on fingerprints of flavones and organic acids in Yinlian Tongfeng Granules by HPLC and clustering analysis, China Pharmacist 17 (2014) 356–359.
[25] M. Erra, I. Moreno, J. Sanahuja, M. Andres, R.F. Reinoso, E. Lozoya, P. Pizcueta, N. Godessart, J.C. Castro-Palomino, Biaryl analogues of teriflunomide as potent DHODH inhibitors, Bioorg. Med. Chem. Lett. 21 (2011) 7268–7272.
[26] J. Chen, C. Wang, J. Wang, L. Cao, Progress in MAPK signaling pathway, China Med. Pharmacy 1 (2011) 32–34.
[27] Y.J. Liang, W.X. Yang, Kinesins in MAPK cascade: How kinesin motors are involved in the MAPK pathway? Gene 684 (2019) 1–9.
[28] Y. Xu, X. Yu, S. Chen, Z. Han, G. Sun, Investigating the effects of Herba Siegesbeckiae on gouty arthritis based on JNK signaling pathway, Chin. J. Osteoporos. 23 (2017) 1340–1345.
[29] A.K. Tausche, K. Richter, A. Grassler, S. Hansel, B. Roch, H.E. Schroder, Severe gouty arthritis refractory to anti-inflammatory drugs: treatment with anti-tumour necrosis factor alpha as a new therapeutic option, Ann. Rheum. Dis. 63 (2004) 1351–1352.
[30] X. Huang, G. Cui, K. Zhou, Correlation of PI3K-Akt signal pathway to apoptosis of tumor cells, Chin. J. Cancer 27 (2008) 331–336.
[31] D. Yu, L. Liu, F. Lu, C. Yang, H. Xue, S. Liu, Effect of total of Dioscoreae Nipponicae Rhizoma on PI3K/AKT signal pathway by in rIL-1β induced fibroblast-like synoviocytes, Chin. J. Exp. Traditional Med. Formulae 18 (2012) 199–202.
[32] R.M. Pope, J. Tschopp, The role of interleukin-1 and the inflammasome in gout: implications for therapy, Arthritis Rheumatism 56 (2007) 3183–3188.
[33] S.A. Jones, K.H. Mills, J. Harris, Autophagy and inflammatory diseases, Immunol. Cell. Biol. 91 (2013) 250–258.
[34] Q. Yang, J. Zhou, Role of autophagy and Toll-like receptor NOD-like receptor signaling pathway in gout inflammation, Chin. J. Rheumatol. 19 (2015) 349–351.